Quenched Disorder and Strain in Crystalline Membranes

Henry Shackleton*
MIT Department of Physics
(Dated: May 19, 2017)

The flat phase of crystalline surfaces has been the focus of recent study, most notably in its applications to graphene. In this paper, we review the foundational concepts of the theory of these low-temperature tethered membranes, focusing on two-dimensional membranes embedded in three-dimensional surfaces. We discuss effects of quenched random disorder and external strain, examining the effects they have on out-of-plane ripples in these membranes.

I. INTRODUCTION

The statistical mechanics of two-dimensional surfaces has long been an area of study. In contrast to one-dimensional polymers, two-dimensional membranes exhibit a variety of behavior depending on their microscopic structure, which leads to a zoo of universality classes. In this paper, we focus on *crystalline* membranes - surfaces with fixed connectivity. These membranes exhibit a flat phase at low temperature and a crumpled phase at high temperature. The transition from one to the other, known as the *crumpling transition*, is accompanied by a change in the radius of gyration and a divergence of specific heat [1]. In this paper, we focus on the low-temperature phase of two-dimensional membranes, where it is appropriate to use a Monge representation to characterize membrane configurations. This low-temperature phase has many applications, most notably of which to graphene [2], which can be described accurately by this low temperature phase. While this flat phase is seemingly a violation of the Mermin-Wagner theorem, we will see that effective long-range interactions allow for this ordering at finite temperature.

II. FREE LOW-TEMPERATURE MEMBRANES

II.1. Monge Representation and Free Energy Equation

We consider a $D = 2$ membrane embedded in a $d = 3$ space, specified by a three dimensional position vector $\mathbf{X}(x^k)$ parameterized by two parameters x^1, x^2. By defining $\mathbf{t}_i = \partial_i \mathbf{X}$ and $\partial_i \partial_j \mathbf{X} = b_{ij}\hat{\mathbf{n}} + \Gamma^k{}_{ij}\mathbf{t}_k$, where $v\hat{b}n$ is a normal vector to the membrane, a general expression for the energy density given a nearly flat membrane is

$$\mathcal{F} = \frac{1}{2}\lambda u_{ii}^2 + \mu u_{ij}^2 + \frac{1}{2}\kappa \mathbf{K}_{ii}^2 - \kappa_G \det(\mathbf{K}_{ij}) \tag{1}$$

where λ and μ are are the Lamé coefficients, and we introduce

$$u_{ij} = (\mathbf{t}_i \cdot \mathbf{t}_j - A_{ij})/2, \ \mathbf{K}_{ij} = b_{ij}\hat{\mathbf{n}} - \mathbf{B}_{ij} \tag{2}$$

and define A_{ij} and $\mathbf{B}_{ij}$ as quenched random tensors[1] indicating a preferred configuration of the system [3]. This can emerge from defects in the material, and can result in low-temperature instabilities [4]. For a flat preferred configuration, $A_{ij} = \delta_{ij}$ and $\mathbf{B}_{ij} = \mathbf{0}$. More generally, our system will have a preferred configuration when A_{ij} and $\mathbf{B}_{ij}$ satisfy the Gauss-Codazzi-Mainardi relations [5], and therefore can be written as

$$A_{ij} = \partial_i \mathbf{X}^0 \cdot \partial_j \mathbf{X}^0, \ \mathbf{B}_{ij} = \partial_i \partial_j \mathbf{X}^0 \tag{3}$$

where the physical meaning of $\mathbf{X}^0$ is the preferred configuration of the material. If A_{ij} and $\mathbf{B}_{ij}$ cannot be written in this form, geometrical frustration becomes manifest. This case has been examined, and by averaging over these quenched random fields via the replica method, we see that this causes a flat disordered phase at $T = 0$ [6]. An interesting note is that the random stress corresponding to A_{ij} is automatically generated through a renormalization group procedure provided non-zero random curvature $\mathbf{B}_{ij}$. For the duration of this paper, we will assume A_{ij} and $\mathbf{B}_{ij}$ can be written in the form of Equation 3.

For small deformations, it is convenient to use the Monge representation

$$\mathbf{X}^0(x, y) = x\hat{\mathbf{e}}_x + y\hat{\mathbf{e}}_y + h(x, y)\hat{\mathbf{e}}_z \tag{4}$$

With this, we can define

$$\mathbf{X} = \mathbf{X}^0 + u_i \hat{\mathbf{t}}_i^0 + f\hat{\mathbf{n}}^0 \tag{5}$$

where $\hat{\mathbf{t}}_i^0 = (\hat{\mathbf{e}}_i + (\partial_i h)\hat{\mathbf{e}}_z)/\sqrt{1 + (\partial_i h)^2}$ is a unit tangent vector and $\hat{\mathbf{n}}^0 = (\hat{\mathbf{e}}_z - \sum_i (\partial_i h)\hat{\mathbf{e}}_i)/\sqrt{1 + \sum_i (\partial_i h)^2}$ is the unit normal vector. For nearly flat surfaces, we can assume $(\partial_i h)^2 \ll 1$ and the metric tensor $g_{ij}^0 \approx \delta_{ij}$, which allows us to simplify [3]

$$\begin{aligned} u_{ij} &= \frac{1}{2}(\partial_i u_j + \partial_j u_i) + \frac{1}{2}\partial_i f \partial_j f - f\partial_i \partial_j h \\ \mathbf{K}_{ij} &= \partial_i \partial_j f \hat{\mathbf{n}}^0 \end{aligned} \tag{6}$$

* hshackle@mit.edu

[1] By 'quenched," we mean that we consider the tensor fixed when averaging over all configurations. This is in contrast to an "annealed" field, which is allowed to change dynamically.

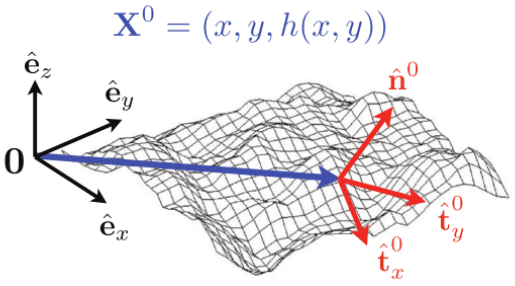

FIG. 1. A reference membrane $\mathbf{X}^0$ described using the Monge representation with respect to Cartesian coordinates.

This reduces Equation 1 to a more tractable form. Upon integrating over the membrane to obtain the free energy of the surface, we see that $\kappa_G \det(\mathbf{K}_{ij})$ can be integrated by parts to a term evaluated on the boundary. This term ultimately relates to the topology of the material, whereas the $\mathbf{K}^2_{ii}$ term relates to out-of-plane deformations within the material. The former term can be neglected for materials where the topology remains constant. The u_{ii} and u_{ij} correspond to in-plane strains, which are coupled to the out-of-plane deformations through terms of the form u^2_{ii} and u^2_{ij}. The final term in u_{ij} depends on the preferred configuration, and vanishes when the preferred configuration is flat ($h = 0$).

II.2. Harmonic Approximation

In the harmonic approximation, we decouple the out-of-plane fluctuations and the in-plane phonon field. With this, Equation 1 reduces to the free energy of a two-dimensional solid [7], plus the out-of-plane displacement field f. This gives the correlation functions

$$\begin{aligned}\langle u_T(\mathbf{q})u_T(\mathbf{q}')\rangle &= \frac{k_BT(2\pi)^2\delta^2(\mathbf{q}+\mathbf{q}')}{\mu q^2}\\ \langle u_L(\mathbf{q})u_L(\mathbf{q}')\rangle &= \frac{k_BT(2\pi)^2\delta^2(\mathbf{q}+\mathbf{q}')}{(2\mu+\lambda)q^2}\\ \langle f(\mathbf{q})f(\mathbf{q}')\rangle &= \frac{k_BT(2\pi)^2\delta^2\left(\mathbf{q}+\mathbf{q}'\right)}{\kappa q^4}\\ &\equiv (2\pi)^2\delta^2(\mathbf{q}+\mathbf{q}')G^0_{ff}(q)\end{aligned} \tag{7}$$

where $G^0_{ff}(q) \sim q^{-4}$ is the propagator of out-of-plane fluctuations in the harmonic approximation. As we will see, this term is modified through couplings between in-plane and out-of-plane fluctuations to its true value $G_{ff}(q) \sim q^{-4+\eta}$.

At this stage, we consider fluctuations in the normals $\mathbf{n}$ of our membrane with respect to the preferred configuration. The angle θ that this normal makes is given by

$$\begin{aligned}\mathbf{n}\cdot\hat{\mathbf{n}}^0 = \cos\theta &= \frac{1}{\sqrt{1+|\vec{\nabla}f|^2}} \approx 1-\frac{1}{2}|\vec{\nabla}f|^2\\ &\approx 1-\frac{1}{2}\theta^2\end{aligned} \tag{8}$$

Fluctuations in the angles between two normals is hence given by

$$\langle\theta(\mathbf{x})\theta(\mathbf{0})\rangle \approx k_BT\int\frac{\mathrm{d}^2\mathbf{q}}{(2\pi)^2}\frac{e^{i\mathbf{q}\cdot\mathbf{x}}+1}{\kappa q^2} = \frac{k_BTC_2(\mathbf{x})}{\kappa} \tag{9}$$

Where $C_2(\mathbf{x})$ is the Coulumb potential in two dimensions, which diverges logarithmically as $\mathbf{x}\to\infty$. Therefore, in accordance with the Mermin-Wagner theorem, long-range order in the normals is destroyed in this two-dimensional membrane.

II.3. Phonon Integration

In order to consider anharmonic corrections, we first integrate out the phonon degrees of freedom and consider the effective free energy. Initially, we consider the simplest case of a defect-free membrane, where $h = 0$. Later, we will detail how these calculations are effected by defects and other modifications.

To integrate out our phonon fluctuations, we decompose u_{ij} into its Fourier modes

$$u^0_{ij} + A^0_{ij} + \sum_{\mathbf{q}\neq 0}\left[\frac{i}{2}\left[q_iu_j(\vec{q})+q_ju_i(\vec{q})\right]+A_{ij}(\vec{q})\right]e^{i\mathbf{q}\cdot\mathbf{x}} \tag{10}$$

where $A_{ij} = \frac{1}{2}\partial_i f\partial_j f$ and the first two terms indicate the $\mathbf{q} = 0$ contribution. By decomposing A into its transverse and longitudinal components, we can integrate out the longitudinal modes by a change of variables [5, 8, 9], and obtain the effective free energy

$$\begin{aligned}F_{eff} &= \frac{1}{2}\kappa\int\mathrm{d}^2x\left(\nabla^2f\right)^2\\ &+\frac{1}{2}K_0\int'\mathrm{d}^2x\left[P^T_{ij}\left[\frac{1}{2}\left(\partial_if\right)\left(\partial_jf\right)\right]\right]^2\end{aligned} \tag{11}$$

where $P^T_{ij} = \delta_{ij} - \partial_i\partial_j/\nabla^2$ is the transverse projection operator, $K_0 = 4\mu(\mu+\lambda)/(2\mu+\lambda)$ is the Young's modulus, and the primed integration indicates that the $\mathbf{q} = 0$ mode has been integrated out. One can see that, by Fourier transforming this expression, one obtains a familiar Gaussian theory with an interaction that mixes up q modes. As will be shown later, this coupling between phonons and out-of-plane fluctuations effectively constitutes a long-range interaction, which allows for long-range order and hence a finite-temperature flat phase without violation of the Mermin-Wagner theorem.

II.4. Self-Consistent Screening Approximation

We proceed by a renormalization procedure to integrate out smaller wavelength modes. Equation 11 can be calculated through an $\epsilon = 4 - D$ expansion [10] where the renormalized stiffness κ and elastic constants scales as $\kappa_R(q) \sim q^{-\eta}$ and $\lambda(q), \mu(q) \sim q^{\eta_u}$, where $\eta = 0.96$ and $\eta_u = 0.08$, with the relation $\eta_u = (4 - D) - 2\eta$. This implies that our momentum-space correlation functions for in-plane and out-of-plane fluctuations scale as $q^{-(\eta_u+2)}$ and $q^{\eta-4}$.

Instead of an ϵ-expansion, we proceed by a *self-consistent screening approximation* (SCSA). This procedure is exact for both large d (to order $1/d$) and for $D = d$. To detail this procedure further, one notes that deriving Equation 11 in a general D-dimensional surface embedded in d-dimensional area results in our interaction term being proportional to $1/(d-D) \equiv 1/d_c$. Expanding in powers of this constitutes expanding in powers of $1/d_c$.

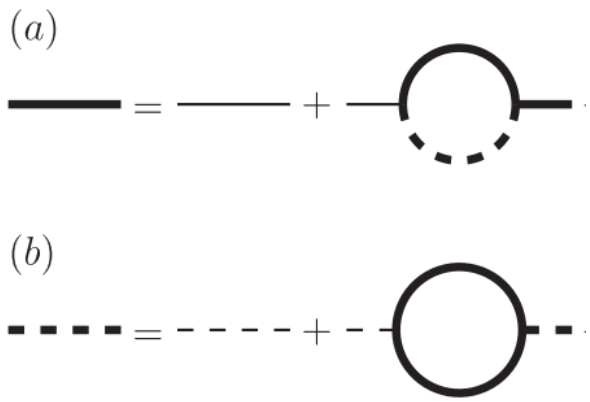

FIG. 2. A diagram representing the SCSA procedure for (a) the renormalized propagator and (b) the renormalized interaction term. Bolded solid (dashed) lines indicate the dressed propagators (interactions). Shown here is a first order SCSA calculation, where we only consider one-loop diagrams [11].

In the approximation we use, we replace instances of our propagator with a dressed propagator (i.e. the propagator with the self-energy factored in), and interactions with screened interactions. This constitutes a partial summation, mixing together different orders of $1/d_c$. As such, this uncontrolled approximation makes it difficult to estimate accuracy. However, comparison to numerical simulations allow us to roughly determine the appropriateness of this approximation.

As illustrated in Figure 2, carrying out this process considering one-loop diagrams gives two coupled equations. Plugging in the ansatz that our propagator $G(q) \sim C/q^{4-\eta}$ for some constant C, we obtain $\eta = 0.821$ [12]. Through the relation $\eta_u = 2 - 2\eta$ (this comes from Ward identities of rotational symmetry, but also falls from the SCSA calculation itself), it follows that $\eta_u = 0.358$. This is compatible with numerical simulations, which predict $\eta = 0.82$ [13], 0.72 [14], and 0.85 [15]. Additionally, by examining Equation 9, we see that our wavelength-dependent rigidity $\kappa_R(q) \sim q^{-\eta}$ allows the correlations between angles of normals to converge to a finite value, thereby permitting a flat phase at non-zero temperature.

II.5. Non-trivial Preferred Configurations

We now examine the case of a non-trivial preferred configuration, detailed in [9]. We assume the height profiles of $\mathbf{X}^0$ are random and take the form [2]

$$\begin{aligned}\overline{h(\mathbf{q})h(\mathbf{q}')} &= \frac{(2\pi)^2\delta^2(\mathbf{q}+\mathbf{q}')\Delta^2}{q^{d_h}} \\ &\equiv (2\pi)^2\delta^2(\mathbf{q}+\mathbf{q}')G_{hh}(\mathbf{q})\end{aligned} \tag{12}$$

where $h(\mathbf{q})$ is the Fourier transform of $h(\mathbf{x})$. The bar over the value indicates a *quenched* averaging over all preferred configurations h. This is different than the *thermal* averaging previously indicated by $\langle\mathcal{O}\rangle$, which involves summing over configurations given a Boltzmann weight. This distinction is important, as it implies that the propagator $G_{hh}(\mathbf{q})$ is not changed under an RG procedure. It is proposed that such configurations could be realized by flash-polymerizing lipid bilayers, or by using rough surfaces of crystals as a reference membrane. Such models could alo be tested via Monte Carlo simulations.

Upon integrating out phonon fluctuations, we see that our effective free energy includes an additional factor from the non-zero h

$$\begin{aligned}F_{eff} &= \frac{1}{2}\kappa\int \mathrm{d}^2x\left(\nabla^2 f\right)^2 \\ &+ \frac{1}{2}K_0\int' \mathrm{d}^2x\left[P^T_{ij}\left[\frac{1}{2}\left(\partial_i f\right)\left(\partial_j f\right) + f\partial_i\partial_j h\right]\right]^2\end{aligned} \tag{13}$$

This perturbation can again be treated with a SCSA approached, illustrated diagrammatically in Figure 3. An additional term corresponding to the effect of the non-zero reference configuration on the self-energy is included. Solving these self-consistent equations allows us to determine the relevance of the random preferred configuration. For $d_h < 4 - \eta$, G_{hh} is irrelevant, the second diagrams dominate the third, and we reacquire the results referenced previously. Hence the random background metric is irrelevant for $d_h < 3.18$ [9].

For $d > 3.18$, the third term in Figure 3 is relevant, and we obtain $\eta = \eta_u = (d_h - 2)/2$. Not only does this change the value of η, but the relation $\eta_u = 2 - 2\eta$ no longer holds due to the relevance of the background metric. This

[2] The exact form of this expression differs from [9]. This is due to convention differences in Fourier transforms, and this paper is follows the convention of [7], where Fourier transforms are passed to the continuum.

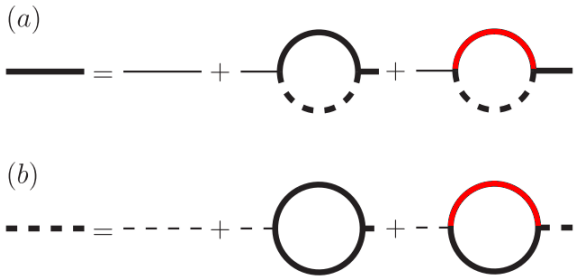

FIG. 3. A diagrammatic representation of the SCSA procedure for quenched random background configurations. As in Figure 2, (a) represents the renormalized propagator and (b) the renormalized interaction term. Bolded solid (dashed) lines indicate the dressed propagators (interactions), and red lines indicate the propagator of the quenched random tensor.

change in scaling exponents is discontinuous, as η and η_u jump from their values given by the free SCSA to $\eta = \eta_u \approx 0.59$ once the background metric is relevant.

III. EXTERNAL FORCES ON MEMBRANES

We now consider the effects of external strain and other forces on our membranes. With regards to strain, there are two different sorts of strain that one can consider - a tangential force inside the boundary, and a strain along the boundary. In these two cases, the free energy gets modified by including terms of the form

$$\int \mathrm{d}^2x \, (\lambda \delta_{ij} a_{ij} + 2\mu a_{ij}) u_{ij} \equiv \int \mathrm{d}^2x \, \tau_{ij} u_{ij} \tag{14}$$

and

$$\oint \mathrm{d}r \, \hat{m}_i \sigma_{ij} u_j \tag{15}$$

respectively. The line integral in Equation 15 corresponds to an integral around the boundary of the membrane, and $\hat{m}_i$ is the normal vector at the boundary. Equation 14 corresponds to some preferred in-plane displacement, potentially arising from electromagnetic forces or viscous drag, whose strength and direction is controlled by a_{ij} [3]. Equation 15 term corresponds to a physical strain along the boundary. We briefly sketch the modifications that each term causes to our membrane.

III.1. In-plane Displacements

With the addition of Equation 14, the correlation function in our harmonic approximation is modified to

$$\langle f(\mathbf{q}) f(\mathbf{q}') \rangle = \frac{k_B T (2\pi)^2 \delta^2(\mathbf{q} + \mathbf{q}')}{q^2 \left(\kappa q^2 + \lambda a_{ii} + 2\mu a_{ij} \frac{q_i q_j}{|\mathbf{q}|^2} \right)} \tag{16}$$

For an isotropic displacement, we can approximate

$$a_{ij} = \frac{\delta A}{2A} \delta_{ij} \equiv u \delta_{ij} \tag{17}$$

where A is the membrane area, and δA is the change due to the induced stress [16]. One can generalize this to other possible strain configurations - a uniaxial strain in the x-direction could be modeled by

$$a_{ij} = \frac{\delta A}{2A} \delta_{ix} \delta_{jx} \equiv v \delta_{ix} \delta_{ij} \tag{18}$$

These possibilities simplify our correlation function to

$$\langle f(\mathbf{q}) f(\mathbf{q}') \rangle = \frac{k_B T (2\pi)^2 \delta^2(\mathbf{q} + \mathbf{q}')}{q^2 \left(\kappa q^2 + 2u(\lambda + \mu) \right)} \tag{19}$$

and

$$\langle f(\mathbf{q}) f(\mathbf{q}') \rangle = \frac{k_B T (2\pi)^2 \delta^2(\mathbf{q} + \mathbf{q}')}{q^2 \left(\kappa q^2 + v(\lambda + 2\mu) \right)} \tag{20}$$

respectively.

When considering an anharmonic theory, the perturbation in Equation 11 obtains a non-trivial addition due to this external strain. However, a simplification can be made when considering materials such as graphene, where the large rigidity κ causes external strain to quickly suppress anharmonic fluctuations. Because of this, we assume that the additional perturbation from the strain will not affect the renormalization of these fluctuations, and we carry out the same SCSA shown in Figure 2. The correction to the propagator $G(\mathbf{q})$, as well as the results from atomistic Monte Carlo simulations using an isotropic strain u, are displayed in Figure 4. One can see that simulations closely mirror calculated values, with accuracy improving as the strain is increased. We hypothesize that this is due to the larger strain causing anharmonic fluctuations to be suppressed more, and thus our previously detailed approximation to be more justified.

While the calculations and simulations in Figure 4 assume a flat preferred configuration ($h = 0$), the assumption of anharmonic suppression should hold for cases of non-trivial preferred configurations. Such a theory would merely constitute an expansion with the SCSA corresponding to the diagrams shown in Figure 3, as opposed to Figure 2.

III.2. Boundary Strain

Considering the effect of strain along the boundary presented in Equation 15, we see that through the Divergence Theorem, the strain along the boundary contributes to the free energy density

$$\frac{\sigma_{ij}}{2} \left(\partial_i u_j + \partial_j u_i \right) \tag{21}$$

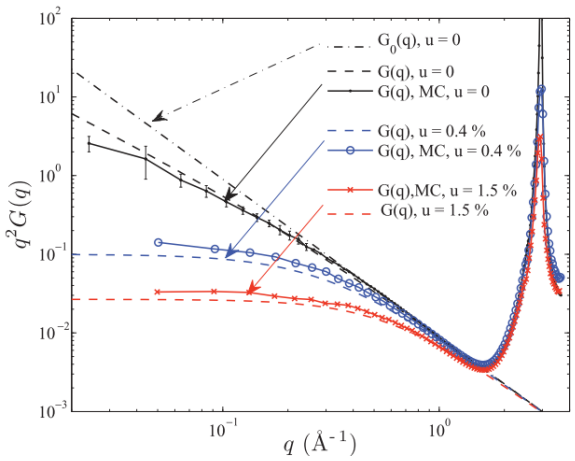

FIG. 4. A graph of of the normal-normal correlation functions $\langle \mathbf{n}(\mathbf{q}\rangle = q^2 G(\mathbf{q})$ calculated from the theory of in-plane strain described (dashed lines) and simulations from atomistic Monte Carlo simulations (solid lines), assuming a flat preferred configuration. Agreement between the two values suggests the disregarding of the strain in the SCSA is valid. [16]

These effect the *derivatives* of phonon displacement, as opposed to the displacements themselves as shown in the earlier section. Note that, while this form is mathematically compatible with the quenched disorder described previously, it most accurately corresponds to the physical case of external strain when $h = 0$, as this form assumes tension as a force on the membrane towards its *preferred configuration*, and physical external tension pulls membranes towards a flat configuration.

Integrating out phonon fluctuations only modifies the Gaussian portion of Equation 11, as opposed to the perturbation. This model can be solved via the SCSA, but the modified form of the propagator G_{ff} means that the SCSA does not lend itself well to clean solutions, especially if one wants to consider general cases of D-dimensional surfaces embedded in d dimensions. In [9], a straightforward RG procedure is carried out to one-loop order to determine the relevance of σ_{ij}. One finds that this term causes κ to scale logarithmically with the length scale upon reaching some critical length scale where the strain suppresses fluctuations, whereas the Young's modulus converges to a fixed value.

The results from this RG procedure can also be used more generally to examine the effects of modifications to the Gaussian theory. Specifically, one sees that higher order gradients in f are irrelevant to one-loop order in this expansion.

III.3. Isotropic Pressure on Membranes

Much work is to be done in the research of crystalline membranes, as there are many external forces that can be considered. A starting point in this investigation would be the examination of a constant pressure p_0 on the membrane, potentially due to the force of gravity. This would correspond to a term of the form $p_0 f$ in our free energy density, as proposed in [3]. However, this poses two problems. Firstly, the form of this additional term as is means that a minimum-energy configuration would correspond to $f = -\infty$. Clearly this is not the sort of system we're interested in - rather, we wish to focus on cases where the surface is *fixed* at the boundary and then exposed to a constant pressure. However, this requires more finer considerations of our boundary conditions than our current theory allows, where we consider boundary terms such as Equation 15 through the Divergence Theorem.

The second issue faced is that the energy term corresponding to this pressure indicates a uniform pressure on the membrane *towards its preferred configuration*, rather than a uniform pressure downward such as gravity. For $h = 0$, these two things correspond exactly, but in general, we wish to have our modified free energy have terms of the form

$$\begin{aligned} p_o\left(\mathbf{X}^0 \cdot \hat{\mathbf{e}}_z\right) &= p_0\left[u_i \frac{\partial_i h}{\sqrt{1+\left(\partial_i h\right)^2}} + f\right] \\ &\approx p_o\left(u_i \partial_i h + f\right) \end{aligned} \tag{22}$$

where the last step assumes $(\partial_i h)^2 \ll 1$. This allows for a coupling between the pressure and the in-plane deformations. By integrating this coupling by parts (the boundary term goes away because, as previously mentioned, we will wish to enforce fixed boundary conditions, i.e. $h(x, y) = 0$ along the boundary), we obtain what can be thought of as a modified Lamé coefficient

$$\lambda_{eff}(x, y) = \lambda + 2 p_o h(x, y) \tag{23}$$

This position-dependent Lamé coefficient suggests a stronger preference towards the minimum energy configuration, as we would expect from a uniform pressure on a non-uniform membrane. It is worth noting that the minimum energy configuration, $\mathbf{X}^0$, is expected to change under this pressure, although determining this is a mechanical problem of balancing forces between the beding rigidity of the membrane and the applied pressure.

IV. CONCLUSIONS

Two-dimensional membranes are of great interest in areas of statistical physics, both for their real-world applications to graphene as well as the wealth of different features they can exhibit. Crystalline structures display a further variety of features depending on the microscopic configurations, as well as external forces. By examining these possibilities and how they modify existing theories, one hopes to gain a more complete understanding of the interplay between the theory two-dimensional surfaces and applications to everyday life.

V. ACKNOWLEDGEMENTS

The author thanks Professor Mehran Kardar for his dedication, commitment, and passion for teaching statistical mechanics. Additionally, the author thanks John Frank for his initial topic suggestions, as well as Alex Seigenfeld, Patrick Ledwith, and Tomohiro Soejima for their technical advice.

[1] M. Paczuski, M. Kardar, and D. R. Nelson, Phys. Rev. Lett **60**, 2638 (1988).
[2] K. V. Zakharchenko, R. Roldán, A. Fasolino, and M. I. Katsnelson, Phys. Rev. B **82** (2010).
[3] A. Košmrlj and D. R. Nelson, Phys. Rev. E **88**, 012136 (2013).
[4] L. Radzihovsky and D. R. Nelson, Phys. Rev. A **44**, 3525 (1991).
[5] D. Nelson, T. Piran, and S. Weinberg, *Statistical Mechanics of Membranes and Surfaces* (2004).
[6] D. C. Morse and T. C. Lubensky, Phys. Rev. A **46**, 1751 (1992).
[7] M. Kardar, *Statistical Physics of Fields* (2007).
[8] S. Sachdev and D. R. Nelson, Journal of Physics C: Solid State Physics **17**, 5473 (1984).
[9] A. Košmrlj and D. R. Nelson, Phys. Rev. E **89** (2014), 1312.4089.
[10] J. A. Aronovitz and T. C. Lubensky, Phys. Rev. Lett. **60**, 2634 (1988).
[11] D. Gazit, Phys. Rev. E **80** (2009).
[12] P. Le Doussal and L. Radzihovsky, Phys. Rev. Lett. **69**, 1209 (1992).
[13] Z. Zhang, H. T. Davis, and D. M. Kroll, Phys. Rev. E **48**, R651 (1993).
[14] Mark J. Bowick, Simon M. Catterall, Marco Falcioni, Gudmar Thorleifsson, and Konstantinos N. Anagnostopoulos, J. Phys. I France **6**, 1321 (1996).
[15] D. Wei and F. Wang, The Journal of Chemical Physics **141**, 144701 (2014).
[16] R. Roldán, A. Fasolino, K. V. Zakharchenko, and M. I. Katsnelson, Phys. Rev. B **83** (2011), 1101.6026.